

Development and optimization by factorial design of polymeric nanoparticles for simvastatin delivery

Dalila Pinto Malaquias¹, Lays Fernanda Nunes Dourado^{1*} , Ângela Maria Quintão Lana² ,
Fernando Souza², José Vilela³, Margareth Andrade³ , Juan Pedro Bretas Roa⁴ ,
Álvaro Dutra de Carvalho-Junior¹  and Elaine Amaral Leite⁵ 

¹*Departamento de Farmácia, Faculdade de Ciências Biológicas e da Saúde, Universidade Federal dos Vales do Jequitinhonha e Mucuri – UFVJM, Diamantina, MG, Brasil*

²*Departamento de Zootecnia, Escola de Veterinária, Universidade Federal de Minas Gerais – UFMG, Belo Horizonte, MG, Brasil*

³*Centro de Tecnologia, SENAI-CETEC, Belo Horizonte, MG, Brasil*

⁴*Departamento de Engenharia Química, Instituto de Ciências e Tecnologia, Universidade Federal dos Vales do Jequitinhonha e Mucuri – UFVJM, Diamantina, MG, Brasil*

⁵*Departamento de Produtos Farmacêuticos, Faculdade de Farmácia, Universidade Federal de Minas Gerais – UFMG, Belo Horizonte, MG, Brasil*

*laysndourado@gmail.com

Abstract

Controlled release systems can modify the release rate of drugs and direct them to specific sites of action, making them more effective and/or reducing the adverse effects. The objective of this study was investigated, poly(β -hydroxybutyrate) (PHB) and poly(ϵ -caprolactone) (PCL) nanospheres to improve the delivery of Simvastatin (SIM). Nanospheres were prepared by the emulsion/evaporation technique of the solvent, varying the amount of SIM added. The SIM quantification was performed using a validated high-performance liquid chromatography method. The average diameter and PDI of formulations without SIM were lower 250 nm and 0.3, respectively. Nanospheres containing 30% of SIM showed values of 265 nm and 0.09, respectively. The average zeta potential was -31.8 mV, suggesting the predominance of repulsive forces that prevent aggregation. *In vitro* release suggest transport occurs by diffusion. Morphological analysis demonstrated spherical particles and rough surfaces. In conclusion, data suggest that PHB/PCL nanospheres are promising delivery systems to SIM.

Keywords: *drug delivery, nanoparticles, PHB, PHB/PCL blend, simvastatin.*

How to cite: Malaquias, D. P., Dourado, L. F. N., Lana, Â. M. Q., Souza, F., Vilela, J. Andrade, M., Roa, J. P. B., Carvalho-Junior, Á. D., & Leite, E. A. (2022). Development and optimization by factorial design of polymeric nanoparticles for simvastatin delivery. *Polímeros: Ciência e Tecnologia*, 32(2), e2022016. <https://doi.org/10.1590/0104-1428.20220016>

1. Introduction

Among the statins, simvastatin (SIM) is a well-known potent competitive inhibitor of 3-hydroxy-3-methylglutaryl coenzyme A (HMG-CoA) reductase, which is the rate-limiting enzyme in cholesterol biosynthesis^[1]. Recent studies have shown that the statins induce osteogenesis and inhibit osteoclastic activity by bone morphogenetic protein 2 (BMP-2)-mediated action; thus, they present an essential role in the development of bone and cartilage^[2,3].

Based on this, SIM would have great potential for fractures and osteoporosis treatment if it reached selectively target to bone^[4-6]. As a Biopharmaceutical Classification System Class II drug, SIM shows low aqueous solubility (0.765 $\mu\text{g}/\text{mL}$ in water at 25°C) and high lipophilicity (log P = 4.68)^[7,8]. Besides extensive hepatic metabolism, studies reported that less than 5% of SIM achieve blood circulation^[9]. To attain the minimum concentration required for the beneficial effects

on bone, high doses of SIM are needed, which might cause toxic effects. Thus, the association of SIM with a new drug delivery system is able to act as a controlled drug delivery system representing a promising alternative for use of SIM in the treatment of many diseases.

Polymeric nanocarriers obtained by processing biodegradable polymers have demonstrated a potential for improving the bioavailability of lipophilic drugs. Among the polymers often used in the pharmaceutical field, poly(β -hydroxybutyrate) (PHB), a linear polyester produced in nature by bacterial fermentation of sugar or lipids, has received special attention due to its biodegradation and biocompatibility properties^[10,11]. However, PHB presents high crystallinity (60 to 90%), which hinders the attack of degrading enzymes; therefore, its degradation occurs slowly^[12,13]. Strategies to alter this property included the development of copolymers

or the blending with another polymer^[14]. Previous studies showed that PHB blends with poly(ϵ -caprolactone) (PCL) were immiscible and incompatible^[15], but PCL reduced the stiffness and improved the processing capacity of the blend as well as increased the biodegradability^[16-18].

Therefore, in this study, the aim was the characterization of nanoparticles of PHB and PCL blends loading SIM in order to obtain a prolonged delivery system capable of improving the biopharmaceutical properties of SIM. Firstly, were prepared nanoparticles unloaded (without drug) and statistical tools were used to evaluate their parameters, like diameter, distribution, and surface charge. After, SIM was added to the nanoparticles (SIM-NP) and the influence of the drug incorporation on the physicochemical properties and nanoparticle stability was observed. Lastly, the drug release behavior from the polymer matrix was studied.

2. Materials and Methods

2.1 Materials

SIM (>99%) was purchased from Fagron (São Paulo, Brazil). PHB (Mw = 600 kDa) was supplied by PHB Industrial S.A. (São Paulo, Brazil). PCL (Mw = 80 kDa) was purchased from Sigma-Aldrich (St. Louis, USA). Chloroform and ethanol were obtained from Labsynth (São Paulo, Brazil). Water was purified using a Milli-Q apparatus (Millipore, Billerica, USA). HPLC grade solvents were purchased from J.T.Baker (Philipsburg, USA). All other chemicals were of analytical grade and were used as received.

2.2 Experimental factorial design

A 2² full factorial design was used in unloaded nanoparticles to determine the influence of two factors: PHB/PCL ratios (A) and the presence or absence of copolymer (B) as well as interactions between them on the following responses: mean diameter, polydispersity index, and zeta potential. Thus, four formulations were prepared in triplicate and named according to the factors employed: PHB/PCL 20/80 and presence copolymer, PHB/PCL 20/80 and absence copolymer, PHB/PCL 80/20 and presence copolymer, and PHB/PCL 80/20 and absence copolymer. Analysis of the effect of each variable on the designated response and possible interactions between the factors was performed using the software SAEG software (Sistema para Análises Estatísticas e Genéticas, version 8.0: Fundação Arthur Bernardes, Viçosa, Brazil).

2.3 Nanoparticle preparation

The copolymer poly(3-hydroxybutyrate-co- ϵ -caprolactone) (PHB-co-CL, Mw = 2kDa) was obtained by transesterification reaction from PHB and PCL and was kindly supplied by Professor Dr. Juan Pedro Bretas Roa according to previous studies^[14].

2.3.1 Blend preparation

Firstly, PHB was solubilized in chloroform at 40°C through constant stirring until complete dissolution of the polymer. For the PCL solubilization in chloroform, only magnetic stirring was used. The polymer solutions were added in different concentrations to obtain PHB/PCL ratios of 20/80 or 80/20. Then, the preparations were diluted in

chloroform at a final concentration of 0.1% (w/w) and were stirred for 2 h and transferred to appropriate glass bottles to avoid solvent evaporation^[14].

2.3.2 Unloaded nanoparticle

All formulations were prepared by the oil-in-water (o/w) emulsion-solvent evaporation method previously described by Suave et al.^[19], but with some modifications.

Briefly, 5 mL of PBH/PCL blend (equivalent to 5 mg of polymer) was added in 45 mL of ethanol in ice bath, and the resulting solution was slowly emulsified in 50 mL of water Milli-Q under constant agitation (9500 rpm, 5 min) with an Ultra Turrax T-25 homogenizer (Ika Labor Technik, Staufen, Germany). Subsequently, the organic solvent was removed by evaporation under reduced pressure at 40°C.

2.3.3 SIM-Nanoparticle

SIM loaded nanoparticles were also prepared as described above using only PHB/PCL blend at ratio 20/80 and named SIM-NP. Briefly, SIM dissolved in chloroform was added simultaneously to blend solution, in different concentrations (10, 15, 20, 25, and 30% of the drug relative to the polymer mass). Non-entrapped SIM was eliminated by centrifugation (Heraeus™ Multifuge™ X1 Centrifuge Series, Thermo Fisher Scientific, Bremen, Germany) at 10,000 rpm at 4°C for 10 min.

2.4 Characterization of the nanoparticles

The average diameter of the particles was determined by unimodal analysis through dynamic light scattering (DLS) at 25°C and a fixed angle of 90°. Samples without prior dilution were transferred to a DTS0012 cell and analyzed in Zetasizer NanoZS90 equipment (Malvern Instruments, Malvern, England). The data reported were particle diameter, and polydispersity index (PDI). Data were expressed as the mean \pm standard deviation (SD) of at least three batches of each formulation.

The zeta potential was evaluated by the electrophoretic mobility determination at the angle of 90° at 25°C. Samples without prior dilution were transferred to a DTS1060C cell and the measurements were performed in triplicate using Zetasizer NanoZS90 equipment (Instruments, Malvern, England). Data were expressed as the mean \pm SD of at least three batches of each formulation.

The quantification of SIM was assessed by high-performance liquid chromatography (HPLC) using previously validated conditions by our group. The chromatographic apparatus of the HPLC analysis consisted of a Model 515 pump, a Model 717 Plus auto-injector, and a Model 2996 variable wavelength UV detector (Waters Instruments, Milford, USA) connected to Empower software. Separations were performed using a 25 cm \times 4 mm, 5 μ m Lichrospher® 100 RP-18 column (Merck Millipore, Darmstadt, Germany). The mobile phase consisted of methanol-phosphoric acid 0.1% (90:10 v/v) mixture, filtered and degassed by suction-filtration through a nylon membrane. The flow rate was 1.2 mL min⁻¹, in isocratic flow, and the injection volume was 20 μ L. The eluate absorbance was monitored at 238 nm. The standard calibration curve was linear over a concentration range of 6.0 - 48.0 μ g/ml and resulted in

the linear equation: $y = 26680x + 42500$, with a correlation coefficient of 0.9992 under our experimental conditions. The quantification of SIM in the nanoparticles was determined before (non-purified SIM-NP) and after (purified SIM-NP) centrifugation. Briefly, the SIM-NP formulations were disrupted using acetonitrile in a volume ratio of 1:2 and later diluted in the mobile phase for HPLC analysis. Data were expressed as the mean \pm SD of at least three batches of each formulation. The encapsulation percentage (EP) was calculated using the following equation: $EP (\%) = [\text{purified SIM-NP}] / [\text{non purified SIM-NP}] * 100$.

Differential scanning calorimetry (DSC) analyses were performed using a DSC 2910 (TA Instruments, New Castle, USA). For DSC measurements, a scan rate of 10°C/min was used at a temperature range of 25-380°C, under nitrogen purge (50 ml/min). For temperature and enthalpy calibration, we used Indium. The lyophilized samples were used for DSC study. Lyophilized SIM-NP4 was obtained using a freeze-drier (Liofilizador LS300, Terroni®, São Paulo, Brazil), after rapid freezing of the formulations into liquid nitrogen. The samples were lyophilized for 24 h at a temperature of -45°C. After freeze-drying, the lyophilized samples were placed directly in aluminum pans and all measurements were made using sealed aluminum pans, and an empty pan was used as a reference. Data acquisition and analysis were performed on a microcomputer using an Isothermal Software Kit provided by TA Instruments (New Castle, USA).

2.5 In Vitro drug release

Initially, the nanoparticles were purified. Membrane (cut-off de 14 kDa, Sigma-Aldrich, EUA) filled with 1 ml of solution, and transferred for a bequer containing Milli Q water at 80°C under agitation. After 30 min, the water was removed, and fresh Milli Q water was introduced once again into the flask and stirred (four wash cycles were performed). To ensure the sink conditions (10% of the saturation concentration) SIM solubility in phosphate-buffered saline (PBS) with 0.1% Tween 80 (w/v) at pH 7.4 was previously determined (5.33 $\mu\text{g}/\text{mL}$). The dissolution/release kinetic study of SIM was investigated by the dialysis method. Briefly, aliquots of 1.0 mL of SIM-NP were enclosed in dialysis bags (cellulose membrane, Mw cut-off of 14,000 kDa, Sigma-Aldrich, St. Louis, USA), incubated in 30.0 mL of PBS buffer (pH 7.4) containing 0.1% Tween 80® at 37°C and maintained under mechanical agitation at 100 rpm. At predetermined time intervals (0, 15, 30, 60, 180, 360, 720, and 1440 min), dialysis bags were removed (n=3 for each time) and the SIM concentration was analyzed by HPLC, as described above. The drug release was calculated by the difference between the initial concentration added and the concentration retained in the dialysis bag. The mechanism of SIM release and dissolution was evaluated by mathematical models.

2.6 Morphological analysis

Atomic Force Microscopy (AFM) was applied to evaluate the morphology and diameter analysis of unloaded nanoparticle composed by PHB/PCL blend at ratio 20/80 without copolymer and SIM-NP. A sample droplet (~10 μL) was deposited on a freshly cleaved mica surface,

spread, and dried with argon flow. The measurements were performed at room temperature, in the air, on a Dimension 3000 and with Multimode Equipment, both monitored by a NanoScope IIIa controller, from Digital Instruments (Santa Barbara, USA). The images were obtained in tapping mode using commercial silicon probes from Nanosensors with cantilevers of 288 μm length, resonance frequencies of 75-98 kHz, and spring constants of 3-7 N/m. The “scan rate” used was 1 Hz. Dimensional analyses were carried out using the “section of analysis” applicative on the system. A minimum of 10 images from each sample was analyzed to assure reproducible results. The values represent the mean \pm SD of at least 40 nanoparticles measurements.

2.7 Stability study

The determination of the storage stability of SIM-NP containing 20% of SIM was performed by storing the formulation at 4°C. Sampling aliquots were taken at 7, 15, and 30 days after preparation to evaluate the following parameters: mean diameter, zeta potential, pH, and drug entrapment. The mean values of these parameters were compared with those obtained at time zero.

2.8 Statistical analysis

The normality and homogeneity of the variance analysis were performed using the Lilliefors’ and Bartlett’s tests, respectively. Unloaded and SIM nanoparticles data were evaluated by the factorial design and linear or multiple regression. The difference among averages was tested using the one-way analysis of variance (ANOVA), followed by the Tukey’s test and was considered significant when P values were lower than 0.05. The statistical software used was SAEG software 8.0.

3. Results

The results of the physicochemical characteristics of the unloaded nanoparticles are shown in Table 1.

In the absence of copolymer, the mean diameter was similar regardless of the polymer ratio used. However, after adding the copolymer, mean diameter values significantly increased were obtained at the highest concentration of PHB (PHB/PCL 80:20). Concerning the PDI values, a significant increase (PDI higher than 0.3) was observed at highest PHB concentration in the presence or absence

Table 1. Physicochemical characteristics of unloaded nanoparticles.

Parameter	PHB/ PCL	Copolymer	
		Absence	Presence
Diameter \pm SD (nm)	20/80	267 \pm 20 Aa	240 \pm 13 Ba
	80/20	252 \pm 23 Ab	46188 \pm 8632 Aa
PDI \pm SD	20/80	0.20 \pm 0.06 Ba	0.15 \pm 0.08 Ba
	80/20	0.45 \pm 0.23 Ab	1.0 Aa
Zeta Potential \pm SD (mV)	20/80	-32.7 \pm 4.1 Ba	-28.9 \pm 0.9 Ba
	80/20	-24.7 \pm 5.2 Aa	-21.9 \pm 4.6 Aa

Data expressed as the mean \pm SD. Mean followed by distinct letters, being small letters on the lines and capital letters in the columns differ within the Tukey’s test ($p < 0.05$). Abbreviations: SD, standard deviation; PDI, polydispersity index.

of copolymer. All formulations showed negative zeta potential values, ranging from -22 to -33 mV. The increase of PHB concentration led to a significant reduction of the zeta potential in the absence or presence of the copolymer.

The interaction effect can be observed in Figure 1. The great slope of lines demonstrates the larger influence of the variable on the system, and the lack of parallelism of lines suggests the interaction between the factors. Thus, there was an interaction between the factors for mean diameter and PDI (Figures 1A, B) values while this effect was not observed for the zeta potential values (Figure 1C).

Taking into account the physicochemical characterization, the formulation containing the lowest ratio of PHB and the absence of copolymer was chosen by subsequent studies to clarify the role of SIM in these parameters.

Then, the influence of different SIM concentrations on the physicochemical parameters: mean diameter, PDI,

zeta potential, and EP of the nanoparticles was evaluated. There was no significant alteration in the mean diameter after increasing SIM concentration, except at 25% of SIM. In addition, PDI values less than 0.3 were obtained for all formulations, characteristic of homogeneous preparations (Figure 2). Besides, no significant change in zeta potential values could be observed after increasing SIM concentration. Values varying from -25 to -38mV were found (data not shown).

The data of EP are shown in Figure 3. The increase in SIM concentration up to 20% gradually increases the EP, and a significant difference could be detected between formulations containing 20 and 10% of the drug.

On the other hand, after adding 30% of SIM, the EP significantly decreased compared to 20% of the SIM. Thus, the highest EP was obtained after adding 20% of SIM. These data were further evaluated by regression analysis, and the third-order polynomial model was the best fit obtained ($r = 0.95$). The maximum point of the parabola obtained at a concentration of 20.25% shows that the developed model describes a behavior close to that obtained experimentally.

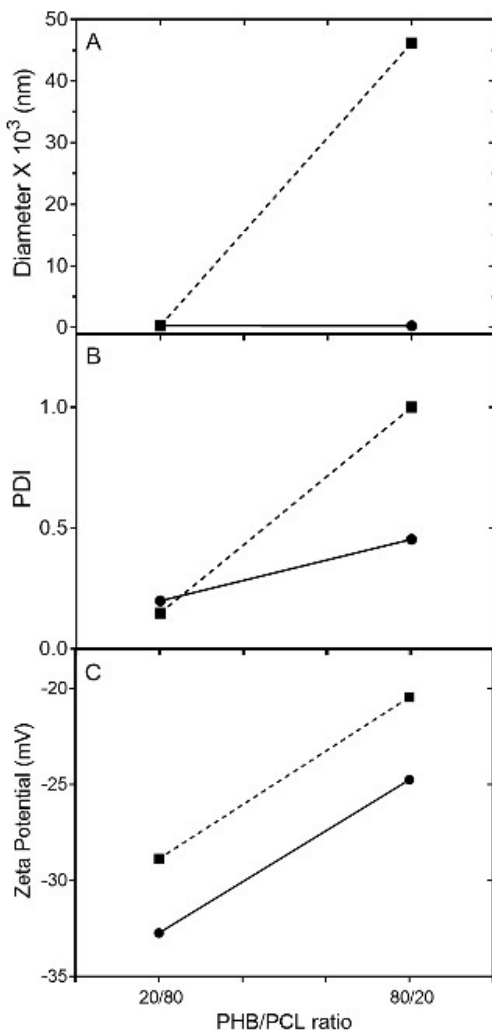


Figure 1. Evaluation of the interaction effect between the polymer proportion and presence (circle) or absence (square) of copolymer on particle diameter (A), PDI (B), and zeta potential (C) values.

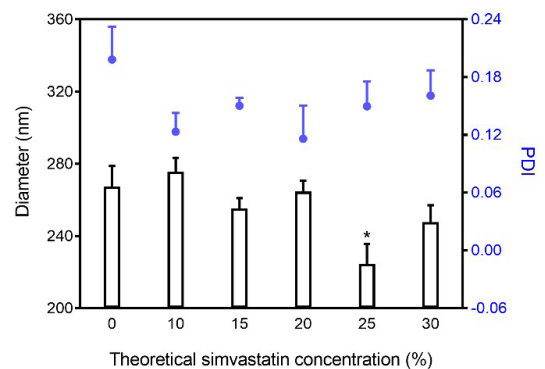


Figure 2. Effect of different concentrations of SIM on the mean diameter (bars) and PDI (blue symbols) of nanoparticles. Asterisk indicates a significant difference compared to formulations 0, 10, and 20%. Data were expressed as the mean \pm SD ($n = 3$), and the level of significance was considered for a p-value < 0.05 .

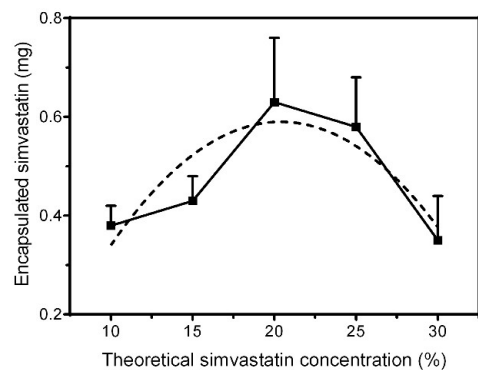


Figure 3. SIM quantity associated with nanoparticles as function of the theoretical SIM concentration. Data were expressed as the mean \pm SD ($n = 3$) and are presented as the continuous line. The dashed line represents the best mathematical model fit.

Due to the highest EP obtained, the formulation containing 20% of SIM was evaluated by the AFM technique. For comparison, unloaded NP was also studied. Both formulations were prepared with PHB/PCL 20/80 without copolymer. The images obtained by AFM demonstrated similar morphology for unloaded NP and SIM-NP, with spherical particles, nanometric size, and large diameter (Figures 4A, B). Both formulations showed spheres with an irregular surface; however, this finding was more pronounced in SIM-NP (Figure 4C), suggesting the presence of SIM on the surface.

A heterogeneous distribution in diameter and height of the nanostructures can also be observed. The 40 particles count in 10 different fields showed a mean diameter of 354 ± 96 nm and a height of 80 ± 39 nm for unloaded NP, while for SIM-NP the values were 244 ± 80 nm and 22 ± 4 nm, respectively. The ratio diameter/height obtained was 4.4 and 11.1 for unloaded and SIM-NP, respectively.

Crystallinity affects several properties of the polymer material, including mechanical, physical, thermodynamic and optical properties. The rate degradation, the affinity and location of the drug in the particle, as well as the mechanism of release, can be influenced by the crystallinity of the polymer used in its preparation^[20]. In view of this, DSC analysis was used to investigate the thermal behavior of the SIM-NP compared to pure components, blend, and physical mixture.

The DSC curve obtained for SIM (Figure 5A) shows an endothermic event at 140°C ($T_{\text{onset}} = 136.5^\circ\text{C}$), which corresponds to the melting point of the drug, which shows its crystalline nature and agrees with previous data described in the literature^[21,22]. For the PHB/PCL blend curve, two peaks at 56°C ($T_{\text{onset}} = 43.6^\circ\text{C}$) and 171°C ($T_{\text{onset}} = 161.5^\circ\text{C}$) were ascribed to the melting point of the PCL and PHB, respectively (Figure 5B).

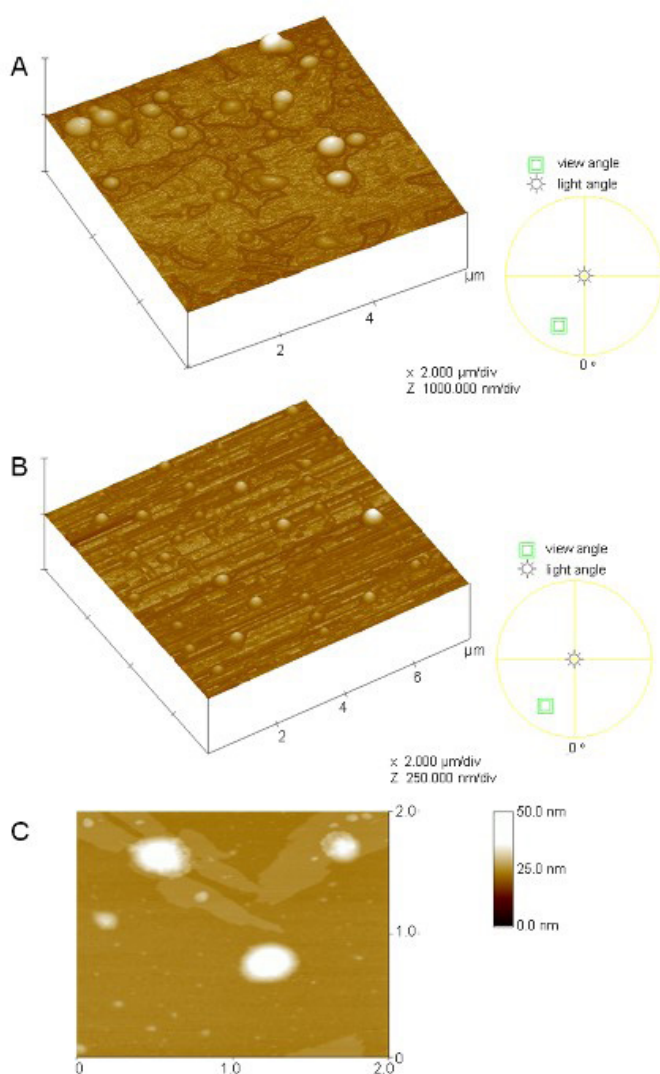


Figure 4. Representative images of unloaded NP (A) and SIM-NP (B) obtained by AFM in a three-dimensional view. In (C), images of SIM-NP. Spheres with irregular surfaces suggesting the drug presence were observed.

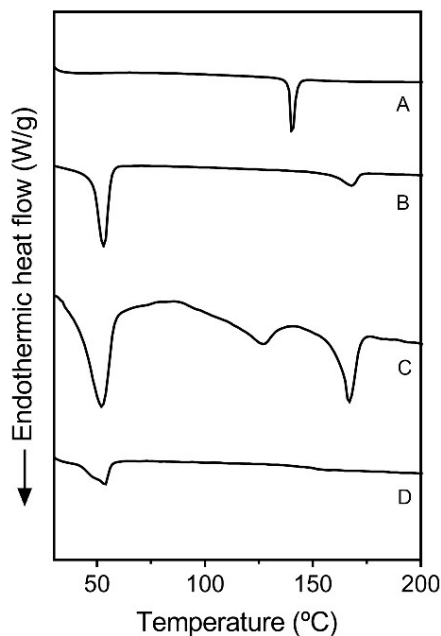


Figure 5. DSC curves obtained under a nitrogen atmosphere and heating ratio of 10 °C/min after analysis of SIM (A), PHB/PCL 20/80 blend (B), physical mixture of the blend and the drug (2:1) (C), and SIM-NP prepared with PHB/PCL 20/80 and 20% of SIM (D).

Similar melting points were observed in other studies that involves PHB/PCL blends^[17,23]. At the physical mixture curve, peaks at 51.5, 127.3, and 166.5° C near values mentioned before were observed (Fig. 5C). On the other hand, in the SIM-NP curve, only a sharp endothermic event at 53.8 °C ($T_{onset} = 42.5$ °C) characteristic of PCL melting point, could be verified. It was possible to observe a meaningful change in the melting event of the SIM, suggesting an interaction between drug and polymers (Figure 5D). The addition of simvastatin provided a reduction in the melting temperature of the polymers, which according to Suave et al.^[19] suggests an affinity of the drug for the polymers. Similar results were described by Kouhi et al.^[23], in PCL nanofibers containing simvastatin. The results obtained showed that the peak referring to the drug disappeared in the DSC curves of the nanofibers containing simvastatin, suggesting that the drug was molecularly dispersed or present in its amorphous form.

The *in vitro* release profiles of SIM and SIM-NP are shown in Figure 6. Initially, SIM-NP showed an initial burst release of 70%, followed by sustained release of more 10% within 12 h. After the period of the test, remains in the systems around 20% of the drug inside the nanosystems. On the other hand, SIM has a low solubility, which can interfere in their *in vitro* release. However, after 750 min approximately 90% of drug could be recovered.

The SIM release kinetics from NP was fitted using zero-order, first-order, and Higuchi mathematical models. Regression coefficients are shown in Table 2. Based on these data, the SIM release from the nanoparticles followed the Higuchi mathematical model which predicts that the release

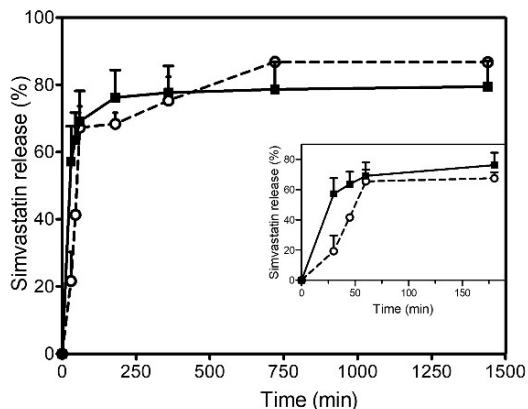


Figure 6. *In vitro* release profile of free SIM (circle) and SIM-NP (square) at 37°C in PBS containing 0.1% Tween 80® pH 7.4. The insert shows the first 180 minutes of release of SIM. Data were expressed as the mean \pm SD (n = 3).

Table 2. Regression coefficients of dissolution/release data of free SIM and SIM loaded NP composed of PHB/PCL 20/80.

Mathematical models	Free SIM	SIM-NP
Zero-order	0.5843	0.3396
First-order	0.4247	0.2819
Higuchi	0.7447	0.5136

occurs by diffusion of the drug through the polymer matrix and/or matrix erosion.

SIM-NP stability was evaluated for a period of 30 days, and the data are presented in Figure 7. As can be seen, there was no significant difference in mean diameter (Figure 7A). Besides, PDI values were lower than 0.2 in all timeframes, suggesting that pharmaceutical preparation did not agglomerate during this period. On the other hand, the amount of SIM-associated with NP was significantly reduced (around 55%) on the seventh day after preparing and keeping on stable after that. The regression analysis of these data showed a significant correlation ($r^2 = 0.99$) in the concentration reduction over time.

The zeta potential values showed a variation of -27 mV to -19mV (Figure 7B), which also showed r^2 higher than 0.9. However, it is noteworthy that the values still were high (near -20mV) suggesting the predominance of repulsive forces that prevent aggregation. Concerning the pH, the values ranging from 5.23 to 5.55, which allows us to suggest that there is no polymeric degradation (Table 3).

4. Discussion

It is well-described that the success of SIM on bone health *in vivo* depends on the local concentration. Finding an appropriate delivery system capable to reduce the drug accumulation in the liver and to deliver to the peripheral tissue has been a great challenge. Polymeric nanoparticles have been employed for carrying insoluble drugs, such as SIM, since their easy production process and application

Table 3. Regression analysis of the data of storage stability.

Parameters	Regression Model	r ²
Diameter	NS	-
Zeta Potential	-26.21 (±1.24) + 0.243 (±0.072) days	0.94
pH	5.27 (±0.07) + 0.011 (±0.004) days	0.80
SIM retention	99.03 (±0.58) – 10.42 (±0.25) days + 0.68 (±0.025) days ² – 0.013 (±0.0005) days ³	0.99

NS: no significant effect.

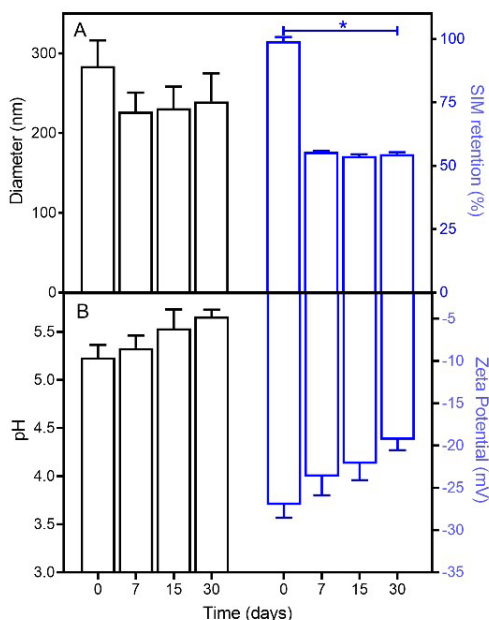


Figure 7. Storage stability evaluation through (A) average diameter (white bars) and retention percentage (blue bars), and (B) pH (white bars) and zeta potential (blue bars) of SIM-NP. Results expressed as the mean ± SD (n = 3). Asterisk indicates a significant difference compared to day 0. The level of significance was considered for a p-value < 0.05.

for several classes of pharmaceutical drugs^[24]. It is known that the formation of the nanoparticles can be influenced by numerous factors, such as the ratio of organic/aqueous phase, solvents, and especially by the polymer used^[25].

Biocompatible and biodegradable polymers are promising for the development of controlled-release formulations^[26-28]. PHB and PCL are some of them, and their degradation leads to the formation of inert, nontoxic, and biocompatible degradation products. Despite being biodegradable, the high crystallinity of PHB provokes a slow degradation, and the polymer might accumulate in the body. Thus, polymer blends have been used as a promising strategy to modify the physicochemical properties and control the drug release profile^[29].

In this study, the effects of the composition (polymer ratio and presence or absence of copolymer) on the physicochemical properties of nanoparticles aiming to optimize a formulation for carrying SIM was evaluated. The data were analyzed using a 2² full factorial design which allowed us to predict possible interactions between variables. This finding has a

significant role in the definition of optimal conditions for formulation development.

The analysis of the influence of polymeric ratio in nanosphere diameter showed particle diameter was similar (p > 0.05) in the absence of copolymer regardless of the polymeric ratio used, as previously described^[30,31]. On the other hand, the increase in PHB concentration led to PDI values higher than 0.3 suggesting heterogeneous samples (Table 1). Although studies have shown that the addition of copolymer may promote higher integration of the phases and increase the interaction between the polymer blend components^[32], in this study, this effect was not observed.

For the highest ratio of PHB even after the addition of copolymer, great and polydisperse particles were formed. In study development by Leimann et al.^[33] similar results were observed in the preparation of Poly(3-hydroxybutyrate-co-3-hydroxyvalerate) (LPHBV) nanoparticles prepared by a miniemulsion/solvent evaporation technique. The increase of the concentration of LPHBV leads to increases in the average particle diameters and polydispersity indexes. According to the literature, this effect can be explained because of increase of the viscosity of the organic phase when higher polymer concentrations are used. Moreover, nanoparticles prepared with higher LPHBV concentrations could coalesced due to the higher viscosity of the organic phase^[34]. Moreover, a great amount of SIM (25%) also can influence the nanoparticles sizes. In a recently published study by our grup^[35], the presence of 25% of SIM in PHB/PPG films led to instability of the PHB/PPG films which, in a way, corroborates the results of this research.

In this sense, the formulation containing PHB/PC 20/80 without copolymer was selected for incorporating SIM. Different concentrations of SIM were evaluated, and the highest EP obtained was 63% when 20% of the drug in relation to polymer mass was used (Figure 3). The low encapsulation efficiency can be explained because of the small superficial area of nanoparticles and the highly insoluble of SIM. An example of this, in a study published by Terukina et al.^[36], PLGA nanospheres showed encapsulation SIM rate of 14.72 ± 0.11%. On the other hand, the encapsulation efficiencies of PLGA microspheres were 89.82 ± 0.78%.

Small and spherical particles with a rough surface were obtained (Figures 2 and 4). It is known that these parameters are strongly influenced by the drug characteristic as well as the technique used in preparing nanoparticles^[37,38]. Previous study has demonstrated that the presence of the roughness on the particle's surface can be associated with the high crystallinity and fast precipitation of PHB, after removing the solvent from the internal phase of the emulsion^[12]. In addition, AFM analysis showed a heterogeneous distribution

of diameter and height. A diameter/height ratio of more than 4 was detected, suggesting that nanoparticles flatten on contact with surfaces^[39].

It's also well-described that the crystallinity may affect the mechanical, physical, thermodynamic, and optical properties of the polymeric material^[40]. According to the literature, many factors can influence the crystallinity of polymers, such as blend polymer and the amount of inorganic component. In study by Ding et al.^[41], the authors observed that silica and calcium additions were both able to decrease the crystallinity of the PHB and PCL blend polymer. This effect was justified by the formation of hydrogen bonding or network formation between the inorganic components phase and polymer matrix.

Thus, DSC analyses were performed in order to evaluate the drug-polymer interactions in the formulation. The addition of SIM reduced the melting temperature of the polymers, suggesting an affinity between the drug and the polymers. The absence of the drug crystallization peak in the SIM-NP curve can suggest that the drug is molecularly dispersed or present in its amorphous form^[42]. Similar results were described in PCL nanofibers containing SIM^[23].

The in vitro release study provides essential information about the physicochemical processes as well as the mechanisms that influence the release rate of the drug. Thus, depending on the release data obtained, changes in preparation conditions, polymer ratio, or drug amount are required to achieve a release profile with desirable characteristics^[43]. Drug release from nanoparticulate systems is dependent on factors like its adsorption on the surface, its diffusion through the polymeric structure, besides the degradation of the polymer^[44]. Drug absorbed on the surface is released faster (burst effect), followed by a slower release of the drug inside the particle. Studies also show slow biodegradation of PCL, and for encapsulating hydrophobic drugs, diffusion is the predominant release form^[45].

The percentage of drug release from SIM-NP was higher in the early hours compared to free drug. The faster release is probably due to decreased polymer crystallinity caused by the association of a small portion of the drug with the matrix. In addition, high release rates have been reported when fatty acid esters are employed in the preparation of microspheres in PLA or PHB blends^[46]. Another important parameter is the drug/polymer ratio. The formation of irregular and porous particles besides phase separation between the drug and polymer due to a large amount of encapsulated drugs often results in a faster release^[47]. The investigation of the release of an insecticide from PHB/PCL microspheres showed that the release rate was favored by the addition of PCL to the blend suggesting the possibility of modulating the release rate by formulating blend^[19]. Therefore, in the present study, it can be proposed that both the release from the nanospheres and SIM occur predominantly by diffusion, but also by erosion of the polymer matrix^[35].

Finally, an acceptable shelf-life is a prerequisite for the successful introduction of this system in therapy. To be considered stable over the period of storage, nanospheres cannot undergo physical or chemical degradation^[48]. In our preliminary storage study, no significant changes were observed in diameter, PDI, and zeta potential.

The maintenance of these parameters may be explained by the electrical repulsion favored by negative zeta values, which could prevent aggregation, improving the stability of the formulations. However, SIM-loaded NP showed a significant reduction ($p < 0.05$) after 7 days of storage. This finding is in accordance with the hypothesis of the absorbed drug on the surface which could be released early.

5. Conclusions

SIM-loaded PHB/PCL nanospheres were successfully manufactured by emulsion/evaporation technique. The results obtained indicate that nanoparticle prepared exhibited a great potential due to high efficiency of encapsulation and stability. Thus, this novel nanostructured carrier system may serve as an encapsulation carrier system for SIM application in bone alterations.

6. Author's Contribution

- **Conceptualization** – Juan Pedro Bretas Roa; Álvaro Dutra de Carvalho-Junior; Elaine Amaral Leite.
- **Data curation** – Álvaro Dutra de Carvalho-Junior.
- **Formal analysis** – Juan Pedro Bretas Roa; Álvaro Dutra de Carvalho-Junior; Elaine Amaral Leite.
- **Investigation** – Dalila Pinto Malaquias; Lays Fernanda Nunes Dourado; Ângela Maria Quintão Lana; Fernando Souza; José Vilela; Margareth Andrade; Juan Pedro Bretas Roa; Álvaro Dutra de Carvalho-Junior; Elaine Amaral Leite.
- **Methodology** – Dalila Pinto Malaquias; Juan Pedro Bretas Roa; Álvaro Dutra de Carvalho-Junior; Elaine Amaral Leite.
- **Project administration** – Álvaro Dutra de Carvalho-Junior.
- **Resources** – Álvaro Dutra de Carvalho-Junior; Elaine Amaral Leite.
- **Software** – NA.
- **Supervision** – Álvaro Dutra de Carvalho-Junior.
- **Validation** – NA.
- **Visualization** – NA.
- **Writing – original draft** – Lays Fernanda Nunes Dourado; Álvaro Dutra de Carvalho-Junior; Elaine Amaral Leite.
- **Writing – review & editing** – Lays Fernanda Nunes Dourado; Álvaro Dutra de Carvalho-Junior; Elaine Amaral Leite.

7. Acknowledgements

Financial supports are provided by Conselho Nacional de Desenvolvimento Científico e Tecnológico (CNPq) and Fundação de Amparo a Pesquisa do Estado de Minas Gerais (FAPEMIG).

7. References

1. Endo, A. (2010). A historical perspective on the discovery of statins. *Proceedings of the Japan Academy. Series B, Physical and Biological Sciences*, 86(5), 484-493. <http://dx.doi.org/10.2183/pjab.86.484>. PMID:20467214.

2. Liu, Y. S., Ou, M. E., Liu, H., Gu, M., Lv, L. W., Fan, C., Chen, T., Zhao, X. H., Jin, C. Y., Zhang, X., Ding, Y., & Zhou, Y. S. (2014). The effect of simvastatin on chemotactic capability of SDF-1 α and the promotion of bone regeneration. *Biomaterials*, 35(15), 4489-4498. <http://dx.doi.org/10.1016/j.biomaterials.2014.02.025>. PMID:24589359.
3. Yue, X., Niu, M., Zhang, T., Wang, C., Wang, Z., Wu, W., Zhang, Q., Lai, C., & Zhou, L. (2016). *In vivo* evaluation of a simvastatin-loaded nanostructured lipid carrier for bone tissue regeneration. *Nanotechnology*, 27(11), 115708. <http://dx.doi.org/10.1088/0957-4484/27/11/115708>. PMID:26881419.
4. Liu, X., Li, X., Zhou, L., Li, S., Sun, J., Wang, Z., Gao, Y., Jiang, Y., Lu, H., Wang, Q., & Dai, J. (2013). Effects of simvastatin-loaded polymeric micelles on human osteoblast-like MG-63 cells. *Colloids and Surfaces. B, Biointerfaces*, 102, 420-427. <http://dx.doi.org/10.1016/j.colsurfb.2012.06.037>. PMID:23006576.
5. Basniwal, P. K., & Jain, D. (2012). Simvastatin: review of updates on recent trends in pharmacokinetics, pharmacodynamics, drug-drug interaction, impurities and analytical methods. *Current Pharmaceutical Analysis*, 8(2), 135-156. <http://dx.doi.org/10.2174/1573412911208020135>.
6. Yin, H., Shi, Z.-G., Yu, Y.-S., Hu, J., Wang, R., Luan, Z.-P., & Guo, D.-H. (2012). Protection against osteoporosis by statins is linked to a reduction of oxidative stress and restoration of nitric oxide formation in aged and ovariectomized rats. *European Journal of Pharmacology*, 674(2-3), 200-206. <http://dx.doi.org/10.1016/j.ejphar.2011.11.024>. PMID:22130356.
7. Lindenberg, M., Kopp, S., & Dressman, J. B. (2004). Classification of orally administered drugs on the World Health Organization Model list of Essential Medicines according to the biopharmaceutics classification system. *European Journal of Pharmaceutics and Biopharmaceutics*, 58(2), 265-278. <http://dx.doi.org/10.1016/j.ejpb.2004.03.001>. PMID:15296954.
8. Jiang, T., Han, N., Zhao, B., Xie, Y., & Wang, S. (2012). Enhanced dissolution rate and oral bioavailability of simvastatin nanocrystal prepared by sonoprecipitation. *Drug Development and Industrial Pharmacy*, 38(10), 1230-1239. <http://dx.doi.org/10.3109/03639045.2011.645830>. PMID:2229827.
9. García, M. J., Reinoso, R. F., Sánchez Navarro, A., & Prous, J. R. (2003). Clinical pharmacokinetics of statins. *Methods and Findings in Experimental and Clinical Pharmacology*, 25(6), 457-481. <http://dx.doi.org/10.1358/mf.2003.25.6.769652>. PMID:12949632.
10. Paulraj, P., Vnootheni, N., Chandramohan, M., & Thevarkattil, M. J. P. (2018). Exploration of Global Trend on Biomedical Application of Polyhydroxyalkanoate (PHA): a patent survey. *Recent Patents on Biotechnology*, 12(3), 186-199. <http://dx.doi.org/10.2174/1872208312666180131114125>. PMID:29384069.
11. Bokrova, J., Marova, I., Matouskova, P., & Pavelkova, R. (2019). Fabrication of novel PHB-liposomes nanoparticles and study of their toxicity in vitro. *Journal of Nanoparticle Research*, 21(3), 49. <http://dx.doi.org/10.1007/s11051-019-4484-7>.
12. Bidone, J., Melo, A. P. P., Bazzo, G. C., Carmignan, F., Soldi, M. S., Pires, A. T. N., & Lemos-Senna, E. (2009). Preparation and characterization of ibuprofen-loaded microspheres consisting of poly(3-hydroxybutyrate) and methoxy poly (ethylene glycol)-b-poly (D,L-lactide) blends or poly(3-hydroxybutyrate) and gelatin composites for controlled drug release. *Materials Science and Engineering C*, 29(2), 588-593. <http://dx.doi.org/10.1016/j.msec.2008.10.016>.
13. Bugnicourt, E., Cinelli, P., Lazzari, A., & Alvarez, V. (2014). Polyhydroxyalkanoate (PHA): review of synthesis, characteristics, processing and potential applications in packaging. *Express Polymer Letters*, 8(11), 791-808. <http://dx.doi.org/10.3144/expresspolymlett.2014.82>.
14. Roa, J. P. B., Mano, V., Faustino, P. B., Felix, E. B., Silva, M. E. S. R., & Souza Filho, J. D. (2010). Síntese e Caracterização do Copolímero Poli(3 Hidroxibutirato co ϵ Caprolactona) A Partir de Poli(3 Hidroxibutirato) e Poli(ϵ Caprolactona). *Polímeros: Ciência e Tecnologia*, 20(3), 221-226. <http://dx.doi.org/10.1590/S0104-14282010005000038>.
15. Gassner, F., & Owen, A. J. (1994). Physical properties of poly(β -hydroxybutyrate)-poly(ϵ -caprolactone) blends. *Polymer*, 35(10), 2233-2236. [http://dx.doi.org/10.1016/0032-3861\(94\)90258-5](http://dx.doi.org/10.1016/0032-3861(94)90258-5).
16. Huang, M.-H., Li, S., Hutmacher, D. W., Coudane, J., & Vert, M. (2006). Degradation characteristics of poly(ϵ -caprolactone)-based copolymers and blends. *Journal of Applied Polymer Science*, 102(2), 1681-1687. <http://dx.doi.org/10.1002/app.24196>.
17. Lovera, D., Márquez, L., Balsamo, V., Taddei, A., Castelli, C., & Müller, A. J. (2007). Crystallization, morphology, and enzymatic degradation of polyhydroxybutyrate/ polycaprolactone (PHB/PCL) blends. *Macromolecular Chemistry and Physics*, 208(9), 924-937. <http://dx.doi.org/10.1002/macp.200700011>.
18. Chee, M. J. K., Ismail, J., Kummerlöwe, C., & Kammer, H. W. (2002). Study on miscibility of PEO and PCL in blends with PHB by solution viscometry. *Polymer*, 43(4), 1235-1239. [http://dx.doi.org/10.1016/S0032-3861\(01\)00725-X](http://dx.doi.org/10.1016/S0032-3861(01)00725-X).
19. Suave, J., Dall'Agno, E. C., Pezzin, A. P. T., Meier, M. M., & Silva, D. A. K. (2010). Biodegradable microspheres of poly(3-hydroxybutyrate)/poly(ϵ -caprolactone) loaded with malathion pesticide: Preparation, characterization, and *in vitro* controlled release testing. *Journal of Applied Polymer Science*, 117(6), 3419-3427. <http://dx.doi.org/10.1002/app.32082>.
20. Huang, J., Wigent, R. J., & Schwartz, J. B. (2006). Nifedipine molecular dispersion in micro particles of ammonio methacrylate copolymer and ethylcellulose binary blends for controlled drug delivery: effect of matrix composition. *Drug Development and Industrial Pharmacy*, 32(10), 1185-1197. <http://dx.doi.org/10.1080/03639040600832827>. PMID:17090441.
21. Oliveira, M. A., Yoshida, M. I., Gomes, E. C. L., Mussel, W. N., Vianna-Soares, C. D., & Pianetti, G. A. (2010). Análise térmica aplicada à caracterização da simvastatina em formulações farmacêuticas. *Química Nova*, 33(8), 1653-1657. <http://dx.doi.org/10.1590/S0100-40422010000800007>.
22. Zhang, Y., Zhang, J., Jiang, T., & Wang, S. (2011). Inclusion of the poorly water-soluble drug simvastatin in mesocellular foam nanoparticles: drug loading and release properties. *International Journal of Pharmaceutics*, 410(1-2), 118-124. <http://dx.doi.org/10.1016/j.ijpharm.2010.07.040>. PMID:20674729.
23. Kouhi, M., Morshed, M., Varshosaz, J., & Fathi, M. H. (2013). Poly (ϵ -caprolactone) incorporated bioactive glass nanoparticles and simvastatin nanocomposite nanofibers: Preparation, characterization and *in vitro* drug release for bone regeneration applications. *Chemical Engineering Journal*, 228, 1057-1068. <http://dx.doi.org/10.1016/j.cej.2013.05.091>.
24. Liechty, W. B., Kryscio, D. R., Slaughter, B. V., & Peppas, N. A. (2010). Polymers for drug delivery systems. *Annual Review of Chemical and Biomolecular Engineering*, 1(1), 149-173. <http://dx.doi.org/10.1146/annurev-chembioeng-073009-100847>. PMID:22432577.
25. Farrag, Y., Montero, B., Rico, M., Barral, L., & Bouza, R. (2018). Preparation and characterization of nano and micro particles of poly(γ -hydroxybutyrate-co- γ -hydroxyvalerate) (PHBV) via emulsification/solvent evaporation and nanoprecipitation techniques. *Journal of Nanoparticle Research*, 20(3), 71. <http://dx.doi.org/10.1007/s11051-018-4177-7>.
26. Makadia, H. K., & Siegel, S. J. (2011). Poly Lactic-co-Glycolic Acid (PLGA) as biodegradable controlled drug delivery carrier. *Polymers*, 3(3), 1377-1397. <http://dx.doi.org/10.3390/polym3031377>. PMID:22577513.

27. Deng, C., Jiang, Y., Cheng, R., Meng, F., & Zhong, Z. (2012). Biodegradable polymeric micelles for targeted and controlled anticancer drug delivery: promises, progress and prospects. *Nano Today*, 7(5), 467-480. <http://dx.doi.org/10.1016/j.nantod.2012.08.005>.
28. Kumari, A., Yadav, S. K., & Yadav, S. C. (2010). Biodegradable polymeric nanoparticles based drug delivery systems. *Colloids and Surfaces. B, Biointerfaces*, 75(1), 1-18. <http://dx.doi.org/10.1016/j.colsurfb.2009.09.001>. PMID:19782542.
29. Yu, L., Dean, K., & Li, L. (2006). Polymer blends and composites from renewable resources. *Progress in Polymer Science*, 31(6), 576-602. <http://dx.doi.org/10.1016/j.progpolymsci.2006.03.002>.
30. Enrico, C., Bartoli, C., Chiellini, F., & Chiellini, E. (2009). Poly(hydroxyalkanoates)-based polymeric nanoparticles for drug delivery. *Journal of Biomedicine & Biotechnology*, 2009, 571702. <http://dx.doi.org/10.1155/2009/571702>. PMID:19789653.
31. Shakeri, F., Shakeri, S., & Hojjatolslami, M. (2014). Preparation and characterization of carvacrol loaded polyhydroxybutyrate nanoparticles by nanoprecipitation and dialysis methods. *Journal of Food Science*, 79(4), N697-N705. <http://dx.doi.org/10.1111/1750-3841.12406>. PMID:24621231.
32. Kim, B. O., & Woo, S. I. (1998). Compatibilizing capability of poly(β -hydroxybutyrate-co- ϵ -caprolactone) in the blend of poly(β -hydroxybutyrate) and poly(ϵ -caprolactone). *Polymer Bulletin*, 41(6), 707-712. <http://dx.doi.org/10.1007/s002890050422>.
33. Leimann, F. V., Cardozo Filho, L., Sayer, C., & Araújo, P. H. H. (2013). Poly(3-hydroxybutyrate-co-3-hydroxyvalerate) nanoparticles prepared by a miniemulsion/solvent evaporation technique: effect of phbv molar mass and concentration. *Brazilian Journal of Chemical Engineering*, 30(2), 369-377. <http://dx.doi.org/10.1590/S0104-66322013000200014>.
34. Musyanovych, A., Schmitz-Wienke, J., Mailänder, V., Walther, P., & Landfester, K. (2008). Preparation of Biodegradable Polymer Nanoparticles by Miniemulsion Technique and Their Cell Interactions. *Macromolecular Bioscience*, 8(2), 127-139. <http://dx.doi.org/10.1002/mabi.200700241>. PMID:18213594.
35. Dourado, L. F. N., Pierucci, A., Roa, J. P. B., & Carvalho Júnior, Á. D. (2021). Assessment of implantable drug delivery technology: poly (3-hydroxybutyrate) / polypropylene glycol films containing simvastatin. *Matéria (Rio de Janeiro)*, 26(04), 1-14. <http://dx.doi.org/10.1590/s1517-707620210004.1389>.
36. Terukina, T., Naito, Y., Tagami, T., Morikawa, Y., Henmi, Y., Prananingrum, W., Ichikawa, T., & Ozeki, T. (2016). The effect of the release behavior of simvastatin from different PLGA particles on bone regeneration *in vitro* and *in vivo* : comparison of simvastatin-loaded PLGA microspheres and nanospheres. *Journal of Drug Delivery Science and Technology*, 33, 136-142. <http://dx.doi.org/10.1016/j.jddst.2016.03.005>.
37. Sinha, V. R., Bansal, K., Kaushik, R., Kumria, R., & Trehan, A. (2004). Poly- ϵ -caprolactone microspheres and nanospheres: an overview. *International Journal of Pharmaceutics*, 278(1), 1-23. <http://dx.doi.org/10.1016/j.ijpharm.2004.01.044>. PMID:15158945.
38. Souto, E. B., Severino, P., & Santana, M. H. A. (2012). Preparação de nanopartículas poliméricas a partir de polímeros pré-formados: parte II. *Polímeros: Ciência e Tecnologia*, 22(1), 101-106. <http://dx.doi.org/10.1590/S0104-14282012005000005>.
39. Montasser, I., Fessi, H., & Coleman, A. W. (2002). Atomic force microscopy imaging of novel type of polymeric colloidal nanostructures. *European Journal of Pharmaceutics and Biopharmaceutics*, 54(3), 281-284. [http://dx.doi.org/10.1016/S0939-6411\(02\)00087-5](http://dx.doi.org/10.1016/S0939-6411(02)00087-5). PMID:12445557.
40. Auras, R. A., Harte, B., Selke, S., & Hernandez, R. (2003). Mechanical, physical, and barrier properties of poly(lactide) films. *Journal of Plastic Film & Sheeting*, 19(2), 123-135. <http://dx.doi.org/10.1177/8756087903039702>.
41. Ding, Y., Roether, J. A., Boccaccini, A. R., & Schubert, D. W. (2014). Fabrication of electrospun poly (3-hydroxybutyrate)/ poly (ϵ -caprolactone)/silica hybrid fibermats with and without calcium addition. *European Polymer Journal*, 55, 222-234. <http://dx.doi.org/10.1016/j.eurpolymj.2014.03.020>.
42. Calvo, P., Vila-Jato, J. L., & Alonso, M. J. (1996). Comparative *in vitro* evaluation of several colloidal systems, nanoparticles, nanocapsules, and nanoemulsions, as ocular drug carriers. *Journal of Pharmaceutical Sciences*, 85(5), 530-536. <http://dx.doi.org/10.1021/js950474+>. PMID:8742946.
43. D'Souza, S. S., & DeLuca, P. P. (2005). Development of a dialysis *in vitro* release method for biodegradable microspheres. *AAPS PharmSciTech*, 6(2), E323-E328. <http://dx.doi.org/10.1208/pt060242>. PMID:16353991.
44. Schaffazick, S. R., Guterres, S. S., Freitas, L. L., & Pohlmann, A. R. (2003). Caracterização e estabilidade físico-química de sistemas poliméricos nanoparticulados para administração de fármacos. *Química Nova*, 26(5), 726-737. <http://dx.doi.org/10.1590/S0100-40422003000500017>.
45. Dash, T. K., & Konkimalla, V. B. (2012). Poly- ϵ -caprolactone based formulations for drug delivery and tissue engineering: a review. *Journal of Controlled Release*, 158(1), 15-33. <http://dx.doi.org/10.1016/j.jconrel.2011.09.064>. PMID:21963774.
46. Schaefer, M. J., & Singh, J. (2002). Effect of tricaprín on the physical characteristics and *in vitro* release of etoposide from PLGA microspheres. *Biomaterials*, 23(16), 3465-3471. [http://dx.doi.org/10.1016/S0142-9612\(02\)00053-4](http://dx.doi.org/10.1016/S0142-9612(02)00053-4). PMID:12099290.
47. Wischke, C., & Schwendeman, S. P. (2008). Principles of encapsulating hydrophobic drugs in PLA/PLGA microparticles. *International Journal of Pharmaceutics*, 364(2), 298-327. <http://dx.doi.org/10.1016/j.ijpharm.2008.04.042>. PMID:18621492.
48. Schaffazick, S. R., Pohlmann, A. R., Freitas, L. L., & Guterres, S. S. (2002). Caracterização e estudo de estabilidade de suspensões de nanocápsulas e de nanoesferas poliméricas contendo diclofenaco. *Latin American Journal of Pharmacy*, 21(2), 99-106. Retrieved in 2022, February 21, from http://www.latamjpharm.org/trabajos/21/2/LAJOP_21_2_1_4_740TAXZEY7.pdf

Received: Feb. 21, 2022

Revised: June 18, 2022

Accepted: July 07, 2022